



A Study of Sonodynamic Therapy of Melanoma C540 Cells in Vitro by Titania/Gold Nanoparticles

Ghazale Perota (MSc)^{1,2}, Parsa Faghani-Eskandarkolaei (MSc Student)¹, Niloofar Zahraie (MSc)^{1,2}, Mohammad Hosein Zare (PhD)³, Naghmeh Sattarahmady (PhD)^{1,2*}

¹Department of Medical Physics and Engineering, School of Medicine, Shiraz University of Medical Sciences, Shiraz, Iran

²Nanomedicine and Nanobiology Research Center, Shiraz University of Medical Sciences, Shiraz, Iran

³Department of Medical Physics, School of Medicine, Shahid Sadoughi University of Medical Science, Yazd, Iran

ABSTRACT

Background: Sonodynamic Therapy (SDT), a safe and non-invasive strategy in tumor therapy, is in development using novel sono-sensitizers, activated by low-intensity ultrasound radiation. SDT mainly progresses through Reactive Oxygen Species (ROS) generation followed by cell annihilation.

Objective: The current study aimed to investigate the effect of ultrasound therapy with titania/gold nanoparticles (NPs) on melanoma cancer.

Material and Methods: In this experimental study, Titania/gold NPs (TGNPs) were synthesized, and their activity was investigated in sonodynamic therapy of a melanoma cancer cell line (C540). SDT was performed at 1.0 W cm⁻² and 1.0 MHz for one minute.

Results: The synthesized NPs that comprised gold NPs of <10 nm into titania NPs of <20 nm showed great stability and cytocompatibility. While TGNPs were biocompatible, a remarkable rate of cell ablation was observed upon ultrasound irradiation due to ROS generation.

Conclusion: The SDT using TGNPs can be introduced as an alternative and low-cost treatment method for melanoma malignancy.

Citation: Perota Gh, Faghani-Eskandarkolaei P, Zahraie N, Zare MH, Sattarahmady N. A Study of Sonodynamic Therapy of Melanoma C540 Cells in Vitro by Titania/Gold Nanoparticles. *J Biomed Phys Eng.* 2024;14(1):43-54. doi: 10.31661/jbpe.v0i0.2310-1674.

Keyword

Malignant Melanoma; Metal Nanoparticles; Gold; Non-Ionizing Radiation; Reactive Oxygen Species

Introduction

Skin cancer is one of the most common malignancies worldwide and melanoma, as a type of the most pernicious ones, originates from the melanocytes [1]. The development of novel and efficient therapeutic methods using various sources of energy that preferably attenuate detrimental effects is a substantial plan in melanoma cancer treatment.

Light-triggered therapy, known as Photodynamic Therapy (PDT), utilizes chemical compounds called photosensitizers for non-invasive therapeutic applications, particularly in the field of oncology [2]. However, two significant limitations of PDT are the inadequate penetration of light into deep tumor tissues, which hinders effective activation of

*Corresponding author:
Naghmeh Sattarahmady
Department of Medical Physics and Engineering,
School of Medicine, Shiraz University of Medical Sciences, Shiraz, Iran
E-mail:
nsattar@sums.ac.ir

Received: 19 October 2023
Accepted: 25 November 2023

the photosensitizer, and the prolonged skin sensitivity caused by the presence of the photosensitizer in cutaneous tissues [2]. Recently, Sonodynamic Therapy (SDT), as a promising and repeatable treatment modality using low-intensity Ultrasound Waves (UW) together with sound-sensitive compounds (sono-sensitizer), has been introduced to overcome the PDT shortcomings [3]. SDT, as a minimally invasive treatment method, works with the effect of UW stimulation on sono-sensitizers [4].

Depending on the frequency, intensity, and exposure time, UW produces both thermal and non-thermal bio-effects. In the thermal mode of SDT, a high-intensity continuous or pulsed UW prompts the thermal effects in the biological tissues [4], while non-thermal interactions of UW radiation with liquid bulks in the tissue prompt the formation of bubbles, named acoustic cavitation. Acoustic cavitation follows with nucleation, growth of bubbles, and near-adiabatic collapsing process. The micro-bubbles represent stable and inertial cavitation based on the UW intensity. In stable cavitation, at lower intensities, the vapor bubbles oscillate around in an equilibrium radius that causes dynamic streaming by the movement of the medium in the environment. Instead, inertial cavitation refers to the expansion of the bubbles to a critical size, leading to a violent collapse at higher intensities [5]. Consequently, the energy diffusion of UW is transformed into enormous amounts of pressure and heat increment in the collapsing bubbles that produce some chemical and physical events, containing micro-jetting, acoustic signals, water pyrolysis, acoustic ablation, and emission of light in a phenomenon called sonoluminescence [6]. Also, the sonoluminescence event is the central trigger of Reactive Oxygen species (ROS) generation, leading to tumor cell ablation [4, 6]. It is assumed that these processes can cause cytoskeleton and cell membrane damage which also enhances the permeability of sono-sensitizers to the target cells [7]. Excessive generation of ROS within cells

can disrupt the balance of redox homeostasis, resulting in cell necrosis or apoptosis. In this line, three mechanisms are dominated for SDT-triggered apoptosis: 1) alteration in expression levels of Bcl-2 family proteins and ROS generation to decrease mitochondrial membrane potential, 2) overloading of calcium ion in the mitochondrial membrane, and 3) up-regulating of intracellular FS7-associated cell surface antigen and its ligand (FAS/FASL) expression [8].

With the emergence of SDT, various sono-sensitizers, such as hematoporphyrin [9] and photofrin [10] have been developed, which have bioavailability limitations due to their hydrophobicity trait and prolonged removal [6]. On the contrary, sensitizers can reduce the level of Glutathione (GSH), which is present at high concentrations within tumor tissue, thereby depleting the protective mechanism against the generated ROS during SDT [11]. Subsequently, modern nanotechnological approaches have been in progress to fabricate novel sono-sensitizers [6]. Hitherto, some different nanostructures such as gold [12, 13], silicon [14], titanium dioxide [13, 15], and oxygen-deficient manganese oxide have been reported as proper sono-sensitizers [16].

Titania (titanium dioxide) is a white, odorless, and non-combustible powder with intrinsic sensitizer properties, chemical inertness for biological tissues, easy fabrication, and low cost [15, 17]. Titania, as a photocatalyst, generates radicals, including superoxide ions ($O_2^{\bullet-}$), singlet oxygen (1O_2), and hydroxyl radicals ($\bullet OH$) by reacting with water during Ultra-violet (UV) exposure and can damage the nearby cells [18]. However, UW is clinically more effective than UV irradiation due to deeper penetration into tumor cells by stimulating sono-sensitizer particles [19]. Despite the fact that the micro-sized particle of titania is considered harmless to animals and people, nanoparticles (NPs) of this material are considered noxious [20]. Up to now, titania NPs have been investigated as an enhancement

agent for radiation therapy, Computed Tomography Imaging (CT) [21], PDT [22], and SDT [19]. Notwithstanding successful application, as a sono-sensitizer, pure titania has some limitations, such as a low quantum yield of ROS due to the fast recombination of electrons and holes (50 ± 30 ns) [23]. Therefore, some noble metals, such as gold, platinum, and silver were presented to combine with titania NPs to increase ROS generation [24].

Among different types of metallic NPs, Au nanomaterials have supernatural importance in nano-biomedical research due to their biocompatibility and stability [13, 25-30]. As a capable sono-sensitizer, Au NPs have been proven to act as nucleation sites for ultrasonic cavitation and decrease the cavitation threshold [31]. Furthermore, the combination of gold with titania preserves electron-hole recombination by trapping the excited electron [24]. Also, AuNPs have been used in diverse investigations, consisting of chemotherapy [13], DNA biosensors [29], Photothermal Therapy (PTT) [32], and imaging [33].

In the present study, titania/gold NPs (TGNPs) were synthesized, and the therapeutic effect of UW combined with TGNPs toward melanoma C540 cells in vitro was investigated.

Material and Methods

Materials

In this experimental study, all the chemical substances and reagents used in this study were obtained from Scharlau Chemie Co. (Spain), Sigma Chemicals Co. (USA), or Merck Co. (Germany). The compounds were employed needless any further purification. Deionized (DI) water was applied all over this study.

Synthesis of TGNPs

A total of 6 mL of Titanium Tetrachloride (TiCl_4) was slowly added into 80 mL of DI water in an ultrasound cleaner bath for 10 min. The obtained mixture that contained a white

powder (hydrated titania NPs) was separated by centrifugation at about 4000 rpm and washed several times with DI water. The powder was then dried at about 70°C followed by calcination for one hour at 450°C to obtain titania NPs. In the next step, 100 mg of titania NPs was completely dispersed in 10 mL of ethanol:water (1:1 V:V) mixture using a probe sonicator followed by addition of 2 mL of 10 mmol L^{-1} HAuCl_4 solution dissolved in the ethanol:water mixture. The resultant dispersion was then stirred for 2 h at 25°C (room temperature). Then, 9 mL of a cooled and 10 mmol L^{-1} NaBH_4 solution was dropwise added into the cooled titania/ HAuCl_4 mixture for about 10 min in an ice bath. The resulting mixture exhibited a dark purple color, and it was stirred for 2 hours. Afterward, the mixture was subjected to centrifugation at approximately 4000 rpm, and the resulting dark purple precipitate, known as TGNPs, was obtained. The TGNPs were then washed multiple times with DI water to remove any impurities.

Characterization of TGNPs

Morphology, size, and composition of TGNPs were investigated using Field Emission Scanning Electron Microscopy (FESEM) with the capability of energy dispersive spectroscopy by a TESCAN Mira 3-XMU (Czech Republic), and Transmission Electron Microscopy (TEM) by a Zeiss-EM10C microscope (Germany) operating at 100 kV. TGNPs powder was placed on a piece of silver adhesive tape followed by gold vapor sputtering to prepare the sample for FESEM. For the TEM sample preparation, a drop of TGNPs suspension in water/acetone (1:1) was placed on a carbon-covered copper grid (400 mesh), and the solvent was evaporated.

Hydrodynamic size, zeta potential, and size distribution of TGNPs were obtained by a SZ-100 - HORIBA instrument (Japan).

Cell culture

C540 (B16/F10) cells of malignant

melanoma were obtained from Pasteur Institute of Iran and cultured in Dulbecco's Modified Eagle Medium (DMEM) supplemented with 10% Fetal Bovine Serum (FBS) and 1% penicillin-streptomycin (10,000 U mL⁻¹). Cell incubation was performed in an atmosphere containing 5% CO₂ with 100% humidity at incubation conditions (37 °C).

Ultrasound exposure setup

The cells were exposed to UW with a Novin ultrasonic apparatus (Iran) with an unfocused planar UW transducer. The center of the UW transducer was placed under the center of each well in contact with the culture plate through a gel. UW had a frequency of 1.0 MHz, an output power of 1.0 W cm⁻², the duty cycle of 100%, and an exposure time of one minute.

Evaluation of toxicity of melanoma cells

To evaluate the toxicity of *C540 (B16/F10)* cells, 1.0×10⁴ cells per well were seeded in 100 µL supplemented DMEM media in each well of microplates for 24 h. Then, the cells were incubated in the presence of different TGNPs concentrations of 0, 5, 25, 50, 100, and 2500 µg mL⁻¹, and cell incubation was continued overnight at incubation conditions. Cells not treated with TGNPs were selected as a control group. The toxicity of the cells was estimated by the MTT proliferation assay. After cell treatment, the cell culture media was replaced with MTT (0.5 mg mL⁻¹, 100 µL in phosphate-buffered saline) followed by incubation for 4 h in the dark at incubation conditions. Then, the MTT solution was entirely discarded followed by adding 100 µL DMSO and incubated for 30 min. After that, the plates were centrifuged at 1800 rpm for 10 min, and the Optical Density (OD) amounts of the supernatants were recorded at 570 nm with a BioTek plate reader (USA). Cell viability was reported as the ratio of OD of each treated group to that of the control one with 100% viability. Measurements were executed in triplicate.

Evaluation of SDT effect of TGNPs on *C540 (B16/F10)* cells

After 24 h of incubation, the cells were firstly treated with selected TGNPs concentrations of 0, 50, and 250 µg mL⁻¹ and then incubated for 4 h at incubation conditions; they were then treated with (or without) UW exposure and finally incubated overnight at incubation conditions. The toxicity of the cells was estimated by the MTT assay. The cells were divided into two groups UW- (without UW exposure) and UW+ (with UW exposure).

Evaluation of SDT effect of TGNPs on intracellular ROS generation

To evaluate the impact of ROS generation upon SDT cytotoxicity, the emission intensity (FI) of Dichlorofluorescein (DCF) was evaluated. After 24 h of incubation, the cells were firstly treated with selected TGNPs concentrations of 0, 50, and 250 µg mL⁻¹, incubated for one hour at incubation conditions, treated with 100 µL of 50 µmol L⁻¹ fresh DCHF-DA solution, and then incubated for 30 min at incubation conditions and finally with (or without) UW exposure. The cells were similarly divided into two groups UW- and UW+. After those steps, the cells were washed three times with phosphate-buffered saline to eliminate the excess DCF. Then, 100 µL of a cell lysis buffer (including NaCl, Triton X-100, and Tris-HCl, at pH=8.0) was added to the wells, and after 30 min, emission intensity at 520 nm was evaluated after excitation at 485 nm using black plates and a plate reader of Biotek (USA).

Statistical analysis

For each quantity, more than three separate experiments were conducted, and non-parametric Kruskal-Wallis and t-tests were used to assess the statistical significance of the outcomes using GraphPad (Prism 8). *P*-values less than 0.05 were accounted for as statistically significant.

Results

Characterization of TGNPs

Figure 1 shows FESEM images recorded at two different magnifications (A, B), an energy

dispersive spectrum (C), and a TEM image of the synthesized TGNPs (D). In the FESEM images, gold, and titania NPs individually appeared as lighter and darker and adhered to each other spots, respectively. TGNPs

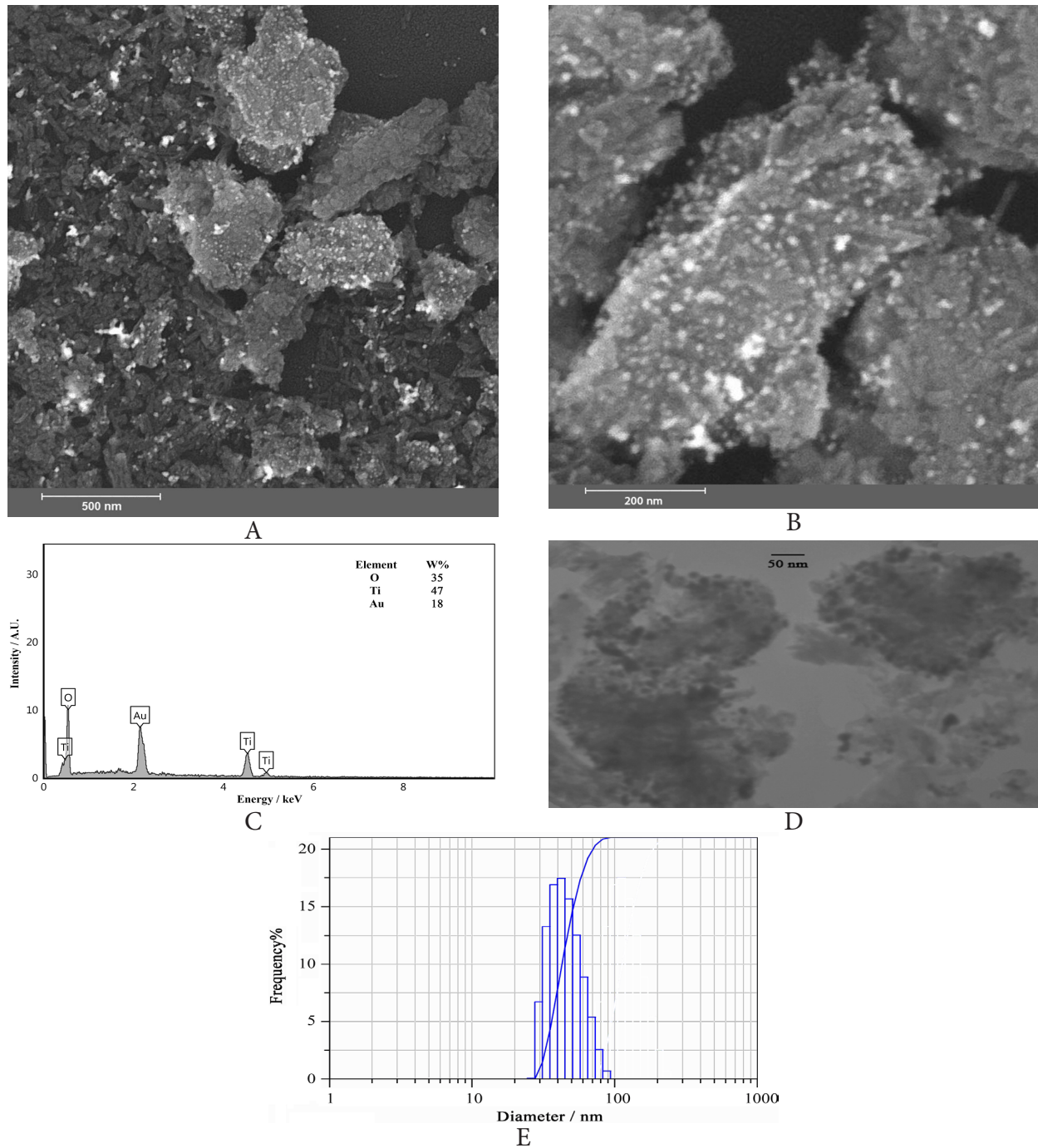


Figure 1: Field emission scanning electron microscopy (FESEM) images recorded at two different magnifications (A, B), an energy dispersive spectrum (C), a transmission electron microscopy (TEM) image (D), and a hydrodynamic size distribution histogram (E) of the synthesized titania/gold nanoparticles.

comprised adhered AU NPs of <10 nm into titania NPs of <20 nm. The spectrum also indicated a TGNPs elemental composition of 47, 35, and 18% by weight for titanium, oxygen, and gold, respectively. This elemental composition denoted a ~4.3/1 (W/W) ratio of titania to gold in TGNPs. The TEM image also confirmed that TGNPs had uniformly distributed gold NPs within the titania ones with near sizes estimated from FESEM images. It should be noted that the TGNPs solution in DI water or PBS was stable without considerable sedimentation or aggregation for at least six months, and the agglomeration observed in the microscopic images was due to drying of the sample before imaging. In Figure 1, a hydrodynamic size distribution histogram for TGNPs is also presented (E). The hydrodynamic size of TGNPs was obtained as 45.4 nm with a polydispersity index of 0.33. These results confirmed the size obtained by electron microscopy and indicated that TGNPs had a narrow size distribution. Given that titania has easy access to the cytomembrane [8] and considering that the pore size of blood vessel endothelium walls typically ranges from approximately 10 nm for normal cells to 10-100

nm for cancer cells, it is plausible that titania particles can penetrate these barriers and interact with the intracellular environment [34]; on the other hand, TGNPs would effectively penetrate the tumor cells. The zeta potential of TGNPs was also measured to be -65.8 mV. The zeta potential absolute value guarantees the dispersion of TGNPs to be stable, and the zeta potential sign leads to limited adsorption of TGNPs by (serum) proteins [35].

Cytotoxicity of TGNPs

Finding a sono-sensitizer with minimum cytotoxicity alone, and maximum cytotoxicity (high responsivity) under UW exposure is crucial for the treatment of malignant cells. Cytotoxicity of TGNPs was evaluated upon 24 h incubation with the C540 cell line, which was treated with different concentrations, and the results of the percentage of the cancer cell viability are presented in Figure 2. Cytotoxicity effects of TGNPs toward C540 cells show a decrement in the cell survival along with an increment in the TGNPs concentration. From these results, the viability of cancer cells treated with a TGNPs concentration as high as 250 $\mu\text{g mL}^{-1}$ was as high as 71%, confirming

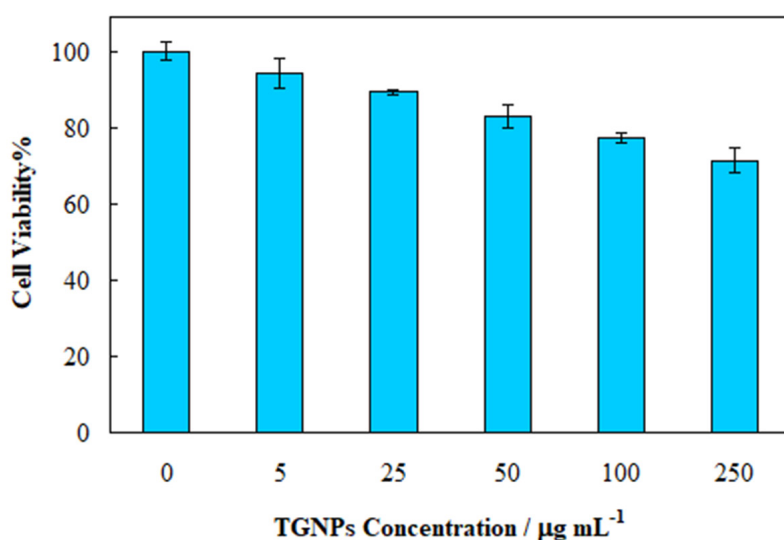


Figure 2: Cytotoxicity of titania/gold nanoparticles toward C540 cells upon 24 h incubation at different concentrations.

biocompatibility of TGNPs. This finding supports previous research indicating that titania-coated Au nanoplates exhibit low cytotoxicity against HeLa cells over a 24-hour period [36].

Cytotoxicity of UW exposure and SDT efficiency of TGNPs

To evaluate the capability of TGNPs for treatment of C540 cells upon UW exposure, the MTT assay was used to measure cellular cell viability after 24 h post-treatment. Samples in UW- and UW+ groups were treated with TGNPs of 50 and 250 $\mu\text{g mL}^{-1}$, and the cell viability percentages are presented in Figure 3. UW exposure of the cells without using TGNPs resulted in a viability decrement to $\sim 90\%$, confirming the biocompatibility of UW exposure and is in line with that reported previously for the C540 cells upon UW exposure [37]. However, Hao et al. reported a viability value of 62% for C6 glioma cells upon UW exposure at 1.0 W cm^{-2} and 1.0 MHz for one minute [38]. Another study showed that the A375 cell-killing ability of UW depended on the time of exposure [39]. It can be decided that the biocompatibility of UW depends on the cell type, and exposure conditions of time, intensity, and frequency [40]. Later, the effective therapeutic frequency of UW was

reported to be in a range of 0.8 to 3.0 MHz [41], and the frequency in a range of 0.5 to 3.0 MHz can produce inertial cavitation inside the tumor [42]. These low frequencies of UW can reversibly open up the strong junction of blood vessel endothelium to break the blood-tumor barrier and help anticancer drugs to transmit [43].

Cell viability of 33% and 69% between the two groups of UW- and UW+ in the presence of 50 and 250 $\mu\text{g mL}^{-1}$ TGNPs, respectively, were observed (with statistically significant differences), and cell viability of $<2\%$ in the presence of TGNPs was obtained with a concentration of 250 $\mu\text{g mL}^{-1}$ upon UW exposure. The findings indicated that UW exposure in combination with TGNPs resulted in a huge reduction in cell viability, compared to cells that were treated with UW irradiation or TGNPs alone.

Intracellular ROS generation evaluation

To assess the generation of ROS during SDT using TGNPs, we quantified the relative FI of treated cells using DCF after excitation at 520 nm. The results of these measurements are presented in Figure 4. The control group, which did not receive TGNPs treatment or UW

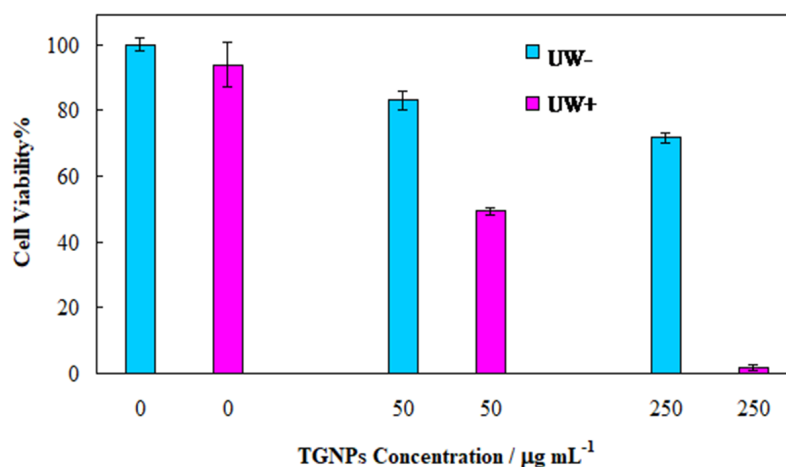


Figure 3: Cytotoxicity of two concentrations of titania/gold nanoparticles of 50 and 250 $\mu\text{g mL}^{-1}$ toward C540 cells upon 24 h incubation without (UW-) or with (UW+) ultrasound exposure.

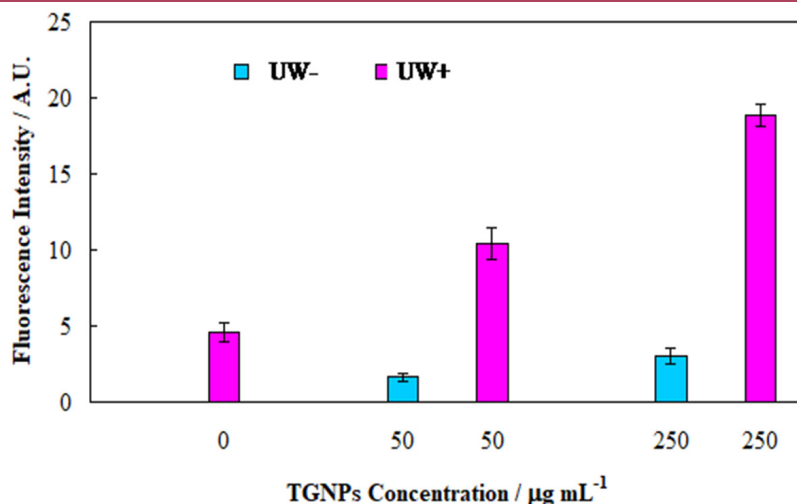


Figure 4: Relative FI after excitation at 520 nm of treated C540 cells with dichlorofluorescein at two concentrations of titania/gold nanoparticles of 50 and 250 $\mu\text{g mL}^{-1}$ without (UW-) or with (UW+) ultrasound exposure.

exposure, exhibited a low FI that served as the baseline signal for comparison. Cell treatment with TGNPs alone (without UW exposure) generated a negligible ROS that supported the low TGNPs cytotoxicity observed for UW-groups in Figure 3. However, FI and intracellular ROS levels significantly increased in the UW+ groups. The observation of a higher level of ROS generation in the presence of TGNPs under UW radiation, compared to UW exposure alone, suggests that TGNPs function as a potent and effective sonosensitizer. Quantitatively, ROS levels under cell SDT using 250 $\mu\text{g mL}^{-1}$ of TGNPs was $\sim 310\%$ greater than cell treatment with UW alone; also, it was $\sim 525\%$ greater than cell treatment with 250 $\mu\text{g mL}^{-1}$ of TGNPs alone. The high level of generated ROS in the UW+ groups induced damage to intracellular proteins and DNA [44] with a higher rate of mortality compared to malignant cells.

Discussion

The use of UW in cancer treatment is increasing worldwide [45]; nonetheless, cavitation thresholds and small therapeutic areas are the main limitations of sonodynamic therapy.

However, the presence of nanomaterials in the treatment medium constructs nucleation sites and dramatically reduces the onset threshold of cavitation [31]. In addition, titania-based nanomaterials have been introduced as effective cavitation promoters that enhance singlet oxygen production [46, 47], albeit with low yield due to fast electron-hole recombination in titania that limits its SDT efficacy [48]. On the other hand, gold, silver, and platinum can enhance the sono-sensitizing efficacy of titania-based nanomaterials [49, 50]. When TGNPs are activated by UW irradiation, it provides a charge transfer channel at the gold/titania interface, and the valence band electrons are excited into the conduction band of titania, leaving the electron holes. Then, due to the lower Fermi level of gold (compared to titania), gold acts as an electron-trap center, resulting in effective inhibition of electron-electron hole recombination [34, 51]. Consequently, the strong interaction between titania and gold NPs leads to the production of $\text{O}_2^{\bullet-}$, $\bullet\text{OH}$, and $^1\text{O}_2$. These generated ROS induce damage to tumor cells by reacting with endogenous or sonosensitizing molecules, resulting in fatal physiological damage through the cre-

ation of ROS [7]. Therefore, administration of TGNPs alone reduced the growth rate of C540 cells, and its combination with UW exposure effectively led to melanoma cell ablation. These findings can be correlated to the ability of titania and gold to generate intracellular ROS.

Conclusion

TGNPs as a cancer therapeutic factor and potential sono-sensitizer along with SDT, were quite well investigated in vitro. Cytotoxicity in the presence of different concentrations of TGNPs demonstrated dose-manner cytotoxicity against the C540 cell line. Also, the generation of ROS was demonstrated in the presence of ultrasound irradiation and TGNPs. Thus, SDT using TGNPs was notably efficient in the treatment of melanoma cancer.

Acknowledgment

We would like to thank the Research Council of the Shiraz University of Medical Science for supporting this research with the grant number “22077”.

Authors' Contribution

Regarding the authors' contributions, N. Sattarahmady conceived the original idea. N. Sattarahmady and MH. Zare supervised the project. G. Perota played a pivotal role in designing the procedure and fabrication of the nanoparticles. G. Perota, P. Faghani-Eskandarkolaei, and N. Zahraie actively participated in data collection, writing, and reviewing the manuscript, ensuring a comprehensive and well-rounded study. All the authors read, modified, and approved the final version of the manuscript.

Ethical Approval

The national ethics committee confirmed the study with the ethical code of IR.SUMS.MED.REC.1399.456. We did not perform any intervention in therapeutic procedures. Therefore, gathering the consent forms was waived

due to the nature of this study.

Conflict of Interest

None

References

1. Seo JO, Yumnam S, Jeong KW, Kim SY. Finasteride inhibits melanogenesis through regulation of the adenylate cyclase in melanocytes and melanoma cells. *J Arch Pharm. Res.* 2018;**41**:324-32. doi: 10.1007/s12272-018-1002-x. PubMed PMID: 29397551. PubMed PMCID: PMC5859039.
2. Nielsen KP, Juzeniene A, Juzenas P, Stamnes K, Stamnes JJ, Moan J. Choice of optimal wavelength for PDT: the significance of oxygen depletion. *J Photochem Photobiol.* 2005;**81**(5):1190-4. doi: 10.1562/2005-04-06-RA-478. PubMed PMID: 15934793.
3. Shibaguchi H, Tsuru H, Kuroki M, Kuroki M. Sonodynamic cancer therapy: a non-invasive and repeatable approach using low-intensity ultrasound with a sonosensitizer. *J Anticancer Res.* 2011;**31**(7):2425-9. PubMed PMID: 21873154.
4. Tachibana K, Feril Jr LB, Ikeda-Dantsuji Y. Sonodynamic therapy. *Ultrasonics.* 2008;**48**(4):253-9. doi: 10.1016/j.ultras.2008.02.003. PubMed PMID: 18433819.
5. Serpe L, Foglietta F, Canaparo R. Nanosonotechnology: the next challenge in cancer sonodynamic therapy. *J Nanotechnol Rev.* 2012;**1**(2):173-82. doi: 10.1515/ntrev-2011-0009.
6. McHale AP, Callan JF, Nomikou N, Fowley C, Callan B. Sonodynamic therapy: concept, mechanism and application to cancer treatment. *Adv Exp Med Biol.* 2016:429-50. doi: 10.1007/978-3-319-22536-4_22. PubMed PMID: 26486350.
7. Rosenthal I, Sostaric JZ, Riesz P. Sonodynamic therapy—a review of the synergistic effects of drugs and ultrasound. *Ultrason Sonochem.* 2004;**11**(6):349-63. doi: 10.1016/j.ultsonch.2004.03.004. PubMed PMID: 15302020.
8. Rengeng L, Qianyu Z, Yuehong L, Zhongzhong P, Libo L. Sonodynamic therapy, a treatment developing from photodynamic therapy. *J Photodiagnosis Photodyn Ther.* 2017;**19**:159-66. doi: 10.1016/j.pdpdt.2017.06.003. PubMed PMID: 28606724.
9. Sun H, Ge W, Gao X, Wang S, Jiang S, Hu Y, et al. Apoptosis-promoting effects of hematoporphyrin monomethyl ether-sonodynamic therapy (HMME-SDT) on endometrial cancer. *PLoS One.* 2015;**10**(9):e0137980. doi: 10.1371/journal.pone.0137980. PubMed PMID: 26367393.

- PubMed PMCID: PMC4569302.
10. Kuroki M, Hachimine K, Abe H, Shibaguchi H, Kuroki M, Maekawa SI, et al. Sonodynamic therapy of cancer using novel sonosensitizers. *J Anticancer Res.* 2007;**27**(6A):3673-7.
 11. Fan H, Yan G, Zhao Z, Hu X, Zhang W, Liu H, et al. A smart photosensitizer–manganese dioxide nanosystem for enhanced photodynamic therapy by reducing glutathione levels in cancer cells. *Angew Chem Int Ed Engl.* 2016;**55**(18):5477-82. doi: 10.1002/anie.201510748. PubMed PMID: 27010667. PubMed PMCID: PMC4971833.
 12. Perota G, Zahraie N, Vais RD, Zare M, Sattarahmady N. Au/TiO₂ nanocomposite as a triple-sensitizer for 808 and 650 nm phototherapy and sonotherapy: Synergistic therapy of melanoma cancer in vitro. *J Drug Deliv Sci Technol.* 2022;**76**:103787. doi: 10.1016/j.jddst.2022.103787.
 13. Zahraie N, Perota G, Vais RD, Sattarahmady N. Simultaneous chemotherapy/sonodynamic therapy of the melanoma cancer cells using a gold-paclitaxel nanostructure. *Photodiagnosis Photodyn Ther.* 2022;**39**:102991. doi: 10.1016/j.pdpdt.2022.102991. PubMed PMID: 35779857.
 14. Osminkina L, Kudryavtsev A, Zinovyev S, Sviridov A, Kargina YV, Tamarov K, et al. Silicon nanoparticles as amplifiers of the ultrasonic effect in sonodynamic therapy. *Bull Exp Biol Med.* 2016;**161**(2):296. doi: 10.1007/s10517-016-3399-x. PubMed PMID: 27388631.
 15. You DG, Deepagan V, Um W, Jeon S, Son S, Chang H, et al. ROS-generating TiO₂ nanoparticles for non-invasive sonodynamic therapy of cancer. *Sci Rep.* 2016;**6**(1):23200. doi: 10.1038/srep23200. PubMed PMID: 26996446. PubMed PMCID: PMC4800401.
 16. Guo Z, Yu Y, Shi L, Liao Y, Wang Z, Liu X, et al. Defect engineering triggers exceptional sonodynamic activity of manganese oxide nanoparticles for cancer therapy. *ACS Appl Bio Mater.* 2022;**5**(9):4232-43. doi: 10.1021/acsabm.2c00445. PubMed PMID: 35952652.
 17. Shi H, Magaye R, Castranova V, Zhao J. Titanium dioxide nanoparticles: a review of current toxicological data. *Part Fibre Toxicol.* 2013;**10**:1-33. doi: 10.1186/1743-8977-10-15. PubMed PMID: 23587290. PubMed PMCID: PMC3637140.
 18. Liu L, Miao P, Xu Y, Tian Z, Zou Z, Li G. Study of Pt/TiO₂ nanocomposite for cancer-cell treatment. *J Photochem Photobiol B.* 2010;**98**(3):207-10. doi: 10.1016/j.jphotobiol.2010.01.005. PubMed PMID: 20149675.
 19. Yamaguchi S, Kobayashi H, Narita T, Kanehira K, Sonezaki S, Kudo N, et al. Sonodynamic therapy using water-dispersed TiO₂-polyethylene glycol compound on glioma cells: comparison of cytotoxic mechanism with photodynamic therapy. *Ultrason Sonochem.* 2011;**18**(5):1197-204. doi: 10.1016/j.ultsonch.2010.12.017. PubMed PMID: 21257331.
 20. Kim D, Yu MK, Lee TS, Park JJ, Jeong YY, Jon S. Amphiphilic polymer-coated hybrid nanoparticles as CT/MRI dual contrast agents. *Nanotechnology.* 2011;**22**(15):155101. doi: 10.1088/0957-4484/22/15/155101. PubMed PMID: 21389582.
 21. Smith L, Kuncic Z, Ostrikov K, Kumar S. Nanoparticles in cancer imaging and therapy. *J Nanomater.* 2012;**2012**:1-7. doi: 10.1155/2012/891318.
 22. Yurt F, Ocakoglu K, Ince M, Colak SG, Er O, Soyulu HM, et al. Photodynamic therapy and nuclear imaging activities of zinc phthalocyanine-integrated TiO₂ nanoparticles in breast and cervical tumors. *Chem Biol Drug Des.* 2018;**91**(3):789-96. doi: 10.1111/cbdd.13144. PubMed PMID: 29136341.
 23. Ozawa K, Emori M, Yamamoto S, Yukawa R, Yamamoto S, Hobara R, et al. Electron–hole recombination time at TiO₂ single-crystal surfaces: Influence of surface band bending. *J Phys Chem Lett.* 2014;**5**(11):1953-7. doi: 10.1021/jz500770c. PubMed PMID: 26273879.
 24. Deepagan V, You DG, Um W, Ko H, Kwon S, Choi KY, et al. Long-circulating Au-TiO₂ nanocomposite as a sonosensitizer for ROS-mediated eradication of cancer. *Nano Lett.* 2016;**16**(10):6257-64. doi: 10.1021/acs.nanolett.6b02547. PubMed PMID: 27643533.
 25. Negahdary M, Heli H. An electrochemical troponin I peptisensor using a triangular icicle-like gold nanostructure. *Biochem Eng J.* 2019;**151**:107326. doi: 10.1016/j.bej.2019.107326.
 26. Heli H, Amirizadeh O. Non-enzymatic glucose biosensor based on hyperbranched pine-like gold nanostructure. *Mater Sci Eng C Mater Biol Appl.* 2016;**63**:150-4. doi: 10.1016/j.msec.2016.02.068. PubMed PMID: 27040206.
 27. Negahdary M, Heli H. An electrochemical peptide-based biosensor for the Alzheimer biomarker amyloid- β (1–42) using a microporous gold nanostructure. *Mikrochim Acta.* 2019;**186**:1-8. doi: 10.1007/s00604-019-3903-x. PubMed PMID: 31713687.
 28. Vais RD, Karimian K, Heli H. Electrooxidation and amperometric determination of vorinostat on hierarchical leaf-like gold nanolayers. *Talanta.* 2018;**178**:704-9. doi: 10.1016/j.talanta.2017.10.001. PubMed PMID: 29136884.

29. Vais RD, Heli H, Sattarahmady N. Label-free electrochemical DNA biosensing of MR TV 29 18s ribosomal RNA gene of *Trichomonas vaginalis* by signalization of non-spherical gold nanoparticles. *Mater Today Commun.* 2023;**34**:105123. doi: 10.1016/j.mtcomm.2022.105123.
30. Heidari M, Sattarahmady N. A review on application of gold nanostructures in cancer therapy. *Basic & Clinical Cancer Res.* 2015;**7**(2&3):32-6.
31. Tuziuti T, Yasui K, Sivakumar M, Iida Y, Miyoshi N. Correlation between acoustic cavitation noise and yield enhancement of sonochemical reaction by particle addition. *J Phys Chem A.* 2005;**109**(21):4869-72. doi: 10.1021/jp0503516. PubMed PMID: 16833832.
32. Kayani Z, Vais RD, Soratijahromi E, Mohammadi S, Sattarahmady N. Curcumin-gold-polyethylene glycol nanoparticles as a nanosensitizer for photothermal and sonodynamic therapies: In vitro and animal model studies. *Photodiagnosis Photodyn Ther.* 2021;**33**:102139. doi: 10.1016/j.pdt.2020.102139. PubMed PMID: 33310015.
33. Malekzadeh R, Ghorbani M, Faghani P, Abdollahi BB, Mortezaazadeh T, Farhood B. Fabrication of targeted gold nanoparticle as potential contrast agent in molecular CT imaging. *J Radiat Res Appl Sc.* 2023;**16**(1):100490. doi: 10.1016/j.jrras.2022.100490.
34. Abdulla-Al-Mamun M, Kusumoto Y, Zannat T, Islam MS. Synergistic enhanced photocatalytic and photothermal activity of Au@TiO₂ nanopellets against human epithelial carcinoma cells. *Phys Chem Chem Phys.* 2011;**13**(47):21026-34. doi: 10.1039/c1cp22683e. PubMed PMID: 22011673.
35. Alexis F, Pridgen E, Molnar LK, Farokhzad OC. Factors affecting the clearance and biodistribution of polymeric nanoparticles. *Mol Pharm.* 2008;**5**(4):505-15. doi: 10.1021/mp800051m. PubMed PMID: 18672949. PubMed PMCID: PMC2663893.
36. Gao F, He G, Yin H, Chen J, Liu Y, Lan C, et al. Titania-coated 2D gold nanoplates as nanoagents for synergistic photothermal/sonodynamic therapy in the second near-infrared window. *Nanoscale.* 2019;**11**(5):2374-84. doi: 10.1039/c8nr07188h. PubMed PMID: 30667014.
37. Martins YA, Fonseca MJ, Pavan TZ, Lopez RF. Bi-functional therapeutic application of low-frequency ultrasound associated with zinc phthalocyanine-loaded micelles. *Int J Nanomedicine.* 2020:8075-95. doi: 10.2147/IJN.S264528. PubMed PMID: 33116519. PubMed PMCID: PMC7586016.
38. Hao D, Song Y, Che Z, Liu Q. Calcium overload and in vitro apoptosis of the C6 glioma cells mediated by sonodynamic therapy (hematoporphyrin monomethyl ether and ultrasound). *Cell Biochem Biophys.* 2014;**70**(2):1445-52. doi: 10.1007/s12013-014-0081-7. PubMed PMID: 25158863. PubMed PMCID: PMC4182584.
39. Rezaei M, Samani RK, Kazemi M, Shanei A, Hejazi S. Induction of a bystander effect after therapeutic ultrasound exposure in human melanoma: In-vitro assay. *Int J Radiat Res.* 2021;**19**(1):183-9. doi: 10.18869/acadpub.ijrr.19.1.183.
40. He Y, Wan J, Yang Y, Yuan P, Yang C, Wang Z, et al. Multifunctional polypyrrole-coated mesoporous TiO₂ nanocomposites for photothermal, sonodynamic, and chemotherapeutic treatments and dual-modal ultrasound/photoacoustic imaging of tumors. *Adv Healthc Mater.* 2019;**8**(9):e1801254. doi: 10.1002/adhm.201801254. PubMed PMID: 30844136.
41. Bohari SP, Aboulkheyr H, Nur E, Johan S, Zianudin N. Low intensity ultrasound induced apoptosis in MCF-7 breast cancer cell lines. *Sains Malays.* 2017;**46**(4):575-81. doi: 10.17576/jsm-2017-4604-09.
42. Sengupta S, Balla VK. A review on the use of magnetic fields and ultrasound for non-invasive cancer treatment. *J Adv Res.* 2018;**14**:97-111. doi: 10.1016/j.jare.2018.06.003. PubMed PMID: 30109147. PubMed PMCID: PMC6090088.
43. Wang JE, Liu YH, Liu LB, Xia CY, Zhang Z, Xue YX. Effects of combining low frequency ultrasound irradiation with papaverine on the permeability of the blood-tumor barrier. *J Neurooncol.* 2011;**102**:213-24. doi: 10.1007/s11060-010-0321-7. PubMed PMID: 20683758.
44. Xu S, Zhou Z, Zhang L, Yu Z, Zhang W, Wang Y, et al. Exposure to 1800 MHz radiofrequency radiation induces oxidative damage to mitochondrial DNA in primary cultured neurons. *Brain Res J.* 2010;**1311**:189-96. doi: 10.1016/j.brainres.2009.10.062. PubMed PMID: 19879861.
45. Trendowski M. Using the promise of sonodynamic therapy in the clinical setting against disseminated cancers. *Chemother Res Pract.* 2015;**2015**:316015. doi: 10.1155/2015/316015. PubMed PMID: 26380110. PubMed PMCID: PMC4562321.
46. Madanshetty SI, Apfel RE. Acoustic microcavitation: Enhancement and applications. *J Acoust Soc Am.* 1991;**90**(3):1508-14. doi: 10.1121/1.401890. PubMed PMID: 1939907.
47. Clement G. Perspectives in clinical uses of high-intensity focused ultrasound. *Ultrasonics.* 2004;**42**(10):1087-93. doi: 10.1016/j.ul-

- tras.2004.04.003. PubMed PMID: 15234170.
48. Xu T, Zhao S, Lin C, Zheng X, Lan M. Recent advances in nanomaterials for sonodynamic therapy. *Nano Res.* 2020;**13**:2898-908. doi: 10.1007/s12274-020-2992-5.
49. Ismail AA, Bahnemann DW. Mesoporous Pt/TiO₂ nanocomposites as highly active photocatalysts for the photooxidation of dichloroacetic acid. *J Phys Chem C.* 2011;**115**(13):5784-91. doi: 10.1021/jp110959b.
50. Murdoch M, Waterhouse G, Nadeem M, Metson J, Keane M, Howe R, et al. The effect of gold loading and particle size on photocatalytic hydrogen production from ethanol over Au/TiO₂ nanoparticles. *Nat Chem.* 2011;**3**(6):489-92. doi: 10.1038/nchem.1048. PubMed PMID: 21602866.
51. Ola O, Maroto-Valer MM. Review of material design and reactor engineering on TiO₂ photocatalysis for CO₂ reduction. *J Photochem Photobiol C.* 2015;**24**:16-42. doi: 10.1016/j.jphotochemrev.2015.06.001.